ARTICLES

Measurements of cross section and asymmetry for $e^+e^- \to b\bar{b}$ and heavy quark fragmentation at KEK TRISTAN

F. Liu,[1] L. M. Chinitz,[2,7] K. Abe,[1] R. E. Breedon,[1,7] Y. Fujii,[1] Y. Kurihara,[1] A. Maki,[1] T. Nozaki,[1] T. Omori,[1] H. Sagawa,[1] Y. Sakai,[1] T. Sasaki,[1] Y. Sugimoto,[1] Y. Takaiwa,[1] S. Terada,[1] P. Kirk,[2] C. P. Cheng,[3] W. X. Gao,[3] W. G. Yan,[3] M. H. Ye,[3] A. Abashian,[4] K. Gotow,[4] M. E. Mattson,[4] L. Piilonen,[4] K. L. Sterner,[4] S. Lusin,[5] C. Rosenfeld,[5] S. Wilson,[5] L. Y. Zheng,[5] C. A. Fry,[6] R. Tanaka,[6] Winston Ko,[7] R. L. Lander,[7] J. Rowe,[7] J. R. Smith,[7] D. Stuart,[7] S. Kanda,[8] S. L. Olsen,[8] K. Ueno,[8] F. Kajino,[9] R. Poling,[10] T. Thomas,[10] T. Aso,[11] K. Miyano,[11] H. Miyata,[11] K. Okubo,[11] M. Oyoshi,[11] M. Shirai,[11] Y. Yamashita,[12] M. H. Lee,[13] F. Sannes,[13] S. Schnetzer,[13] R. Stone,[13] J. Vinson,[13] A. Bodek,[14] B. J. Kim,[14] T. Kumita,[14] Y. K. Li,[14] C. Velisarris,[14] R. C. Walker,[14] S. Kobayashi,[15] A. Murakami,[15] S. K. Sahu,[15] M. E. Zomorrodian,[15] Y. S. Chung,[16] D. K. Cho,[16] J. S. Kang,[16] D. Y. Kim,[16] K. B. Lee,[16] K. W. Park,[16] S. K. Kim,[17] S. S. Myung,[17] S. K. Choi,[18] D. Son,[18] S. Ebara,[19] S. Matsumoto,[19] N. Takashimizu,[19] and T. Ishizuka,[20]

(AMY Collaboration)

[1] *KEK, National Laboratory for High Energy Physics, Ibaraki 305, Japan*
[2] *Louisiana State University, Baton Rouge, Louisiana 70803*
[3] *Institute of High Energy Physics, Beijing 100039, China*
[4] *Virginia Polytechnic Institute and State University, Blacksburg, Virginia 24061*
[5] *University of South Carolina, Columbia, South Carolina 29208*
[6] *SSC Laboratory, Dallas, Texas 75237*
[7] *University of California, Davis, California 95616*
[8] *University of Hawaii, Honolulu, Hawaii 96822*
[9] *Konan University, Kobe 658, Japan*
[10] *University of Minnesota, Minneapolis, Minnesota 55455*
[11] *Niigata University, Niigata 950-21, Japan*
[12] *Nihon Dental College, Niigata 951, Japan*
[13] *Rutgers University, Piscataway, New Jersey 08854*
[14] *University of Rochester, Rochester, New York 14627*
[15] *Saga University, Saga 840, Japan*
[16] *Korea University, Seoul 136-701, South Korea*
[17] *Seoul National University, Seoul 151-742, South Korea*
[18] *Kyungpook National University, Taegu 702-701, South Korea*
[19] *Chuo University, Tokyo 112, Japan*
[20] *Saitama University, Urawa 338, Japan*

(Received 4 November 1993)

Using 773 muons found in hadronic events from 142 pb^{-1} of data at a c.m. energy of 57.8 GeV, we extract the cross section and forward-backward charge asymmetry for the $e^+e^- \to b\bar{b}$ process, and the heavy quark fragmentation function parameters for the Peterson model. For the analysis of the $e^+e^- \to b\bar{b}$ process, we use a method in which the behavior of the c quark and lighter quarks is assumed, with only that of the b quark left indeterminate. The cross section and asymmetry for $e^+e^- \to b\bar{b}$ are found to be $R_b = 0.57 \pm 0.06(\text{stat}) \pm 0.08(\text{syst})$ and $A_b = -0.59 \pm 0.09 \pm 0.09$, respectively. They are consistent with the standard model predictions. For the study of the fragmentation function we use the variable $\langle x_E \rangle$, the fraction of the beam energy carried by the heavy hadrons. We obtain $\langle x_E \rangle_c = 0.56^{+0.04+0.03}_{-0.05-0.03}$ and $\langle x_E \rangle_b = 0.65^{+0.06+0.05}_{-0.04-0.06}$, respectively. These are in good agreement with previously measured values.

PACS number(s): 13.65.+i, 13.87.Fh

I. INTRODUCTION

In e^+e^- annihilation multihadron events, the presence of muons is a good marker for the production of heavy quarks. Moreover, since secondary production of heavy quark pairs is strongly suppressed in jet evolution, such muons emerge mainly from the original annihilation.

The electroweak sector of the standard model classi-

fies quarks and leptons into left-handed doublets and right-handed singlets in the weak isospin representation, and makes absolute predictions for the cross section and forward-backward charge asymmetry for the process $e^+e^- \to f\bar{f}$ (where f is either a quark or a lepton). While these predictions have been tested with good precision in lepton-pair production, measurements of quark-pair production suffer from the experimental difficulty of identifying the quark species. In addition, we still are at a stage where the validity of the electroweak theory cannot be established in the quark sector alone. It is an important test of the standard model to verify that the properties of the b quark are consistent with the interpretation of the b quark as a $T_3 = -1/2$ member of a $(t\ b)_L$ weak isospin doublet. The presence of $B^0\bar{B}^0$ mixing reduces the observable asymmetry from the prediction of only the Born term. This relation must be investigated experimentally. Any deviation from the combined prediction of electroweak theory and the $B^0\bar{B}^0$ mixing can be an important signal of a new phenomenon.

The details of how the quarks turn into hadrons after being pair produced in e^+e^- annihilation are in the domain of nonperturbative QCD and are still far from being treated in a rigorous framework. This is especially true for the case of the lighter quarks. On the other hand, it is well established experimentally that hadrons formed from heavy quarks after they are pair produced in an e^+e^- annihilation carry a large fraction of the original quark's energy. Even though this "hard fragmentation" of the heavy quarks is in good qualitative agreement with QCD-inspired models, a fundamental difference exists between experimentally observable quantities and theoretically meaningful quantities. While theoretical models treat only the primordial fragmentation processes, the observed multihadron events contain initial state radiation and hard gluon radiation which make it impossible to determine directly the energies of heavy quarks. Further measurements are useful in this investigation. The data reported here are based on a total integrated luminosity of 142 pb^{-1}. Results from earlier data have been presented previously [1].

This paper discusses the studies of heavy quarks done at the AMY detector at KEK TRISTAN using multihadron events including muons. We present a measurement of the cross section and asymmetry for the process $e^+e^- \to b\bar{b}$, and a measurement of the fragmentation functions for b and c quarks.

II. $e^+e^- \to b\bar{b}$ CROSS SECTION AND ASYMMETRY

The differential cross section for $e^+e^- \to b\bar{b}$ is given as [2]

$$\frac{d\sigma}{d\cos\theta} = \frac{\pi\alpha^2}{2s}\{3[\tfrac{1}{2}\beta_b(3-\beta_b^2)R_b^{VV}(1+C_{\rm QCD}^{VV}) + \beta_b^3 R_b^{AA}(1+C_{\rm QCD}^{AA})](1+\cos^2\theta) + \tfrac{8}{3}\beta_b^2 R_b^{VA}(1+C_{\rm QCD}^{VA})\cos\theta\}, \quad (1)$$

where α is the fine structure constant; s is the square of the c.m. energy; Q_b is the charge of the b quark; β_b is the velocity of b quark; the R's are cross sections in units of $\sigma(e^+e^- \to \mu^+\mu^-)$ for VV, AA, and VA couplings; and χ is the contribution from the Z^0 peak. They are given by

$$R_b^{VV} = Q_b^2 - 8Q_b v_e v_b \mathrm{Re}(\chi) + 16(v_e^2+a_e^2)v_b^2|\chi|^2, \quad (2)$$

$$R_b^{AA} = 16(v_e^2+a_e^2)a_b^2|\chi|^2, \quad (3)$$

$$R_b^{VA} = 3[-6Q_b a_e a_b \mathrm{Re}(\chi) + 48 v_e v_b a_e a_b|\chi|^2], \quad (4)$$

$$\chi = \frac{1}{16\sin^2\theta_W\cos^2\theta_W}\frac{s}{(s-M_Z^2+i\Gamma_Z M_Z)}. \quad (5)$$

The QCD corrections are expanded in terms of α_s/π as

$$C_{\rm QCD}^{VV(AA)} = C_1^{VV(AA)}\left[\frac{\alpha_s}{\pi}\right] + C_2^{VV(AA)}\left[\frac{\alpha_s}{\pi}\right]^2, \quad (6)$$

$$C_{\rm QCD}^{VA} = C_1^{VA}\left[\frac{\alpha_s}{\pi}\right]. \quad (7)$$

At TRISTAN energies, the effect of the b quark mass on the asymmetry and R ratio for $e^+e^- \to b\bar{b}$ is at most 1.5% and can safely be ignored. Thus, the coefficients are given by [3]

$$C_1^{VV(AA)} = 1.0, \quad (8)$$

$$C_2^{VV(AA)} = 1.986 - 0.115N_f = 1.41, \quad (9)$$

$$C_1^{VA} = 0. \quad (10)$$

In our analysis, we correct the resulting R ratio and the asymmetry for the QCD contribution, so that the results can be directly compared with the pure electroweak predictions. They are given by

$$R_b = 3[R_b^{VV} + R_b^{AA}] = 3[Q_b^2 - 8Q_b v_e v_b \mathrm{Re}(\chi) + 16(v_e^2+a_e^2)(v_b^2+a_b^2)|\chi|^2], \quad (11)$$

$$A_b = R_b^{VA}/R_b. \quad (12)$$

With these definitions of R_b and A_b, the differential cross section

$$\frac{d\sigma}{d\cos\theta} = \frac{\pi\alpha^2}{2s}R_b\left[1+\cos^2\theta+\frac{8}{3}A_b\cos\theta\right] \quad (13)$$

is for the pure electroweak process $e^+e^- \to b\bar{b}$. As can be seen in Eqs. (4) and (12), the asymmetry A_b at TRISTAN energies, where the $\mathrm{Re}(\chi)$ term dominates, strongly depends on a_b, which in the standard model is simply T_{3L}. However, at energies reached at the CERN e^+e^- collider LEP, $|\chi|^2$ dominates and the asymmetry is a measure of $v_b a_b$ and is sensitive to $\sin^2\theta_W$.

III. c AND b QUARK FRAGMENTATION FUNCTIONS

Heavy quark systems are the simplest systems in which to study the hadronization mechanism because the production of heavy quark pairs during jet formation is strongly suppressed so they mainly originate directly from the annihilation. This constrains the kinematics of the fragmentation processes. In the fragmentation of

a heavy quark Q,

$$Q \to (Q\bar{q}) + q, \tag{14}$$

the distribution of the fraction of the parent quark's energy that is transferred to the primary hadron $(Q\bar{q})$ is parametrized by a fragmentation function $f_Q(z)$, where z is the energy fraction defined as

$$z = \frac{(E + p_{\parallel})_{\text{hadron}}}{(E + p_{\parallel})_Q}. \tag{15}$$

Fragmentation functions are expected to scale with energy and depend only on the quark flavor.

One of the most commonly used fragmentation functions is that of Peterson *et al.* [4]:

$$f_Q(z) \propto \frac{1}{z[1 - 1/z - \epsilon_Q/(1-z)]^2}, \tag{16}$$

where ϵ_Q is a free parameter to be determined experimentally for each heavy quark. This parameter is expected to scale among heavy flavors like $\epsilon_Q \sim 1/M_Q^2$. Thus, naively, one expects a relation $\epsilon_b/\epsilon_c \approx 1/10$ to hold. However, this is only valid provided the value of z can be determined for each event. Since this is not possible, we have instead used the variable $x_E = E_{\text{hadron}}/E_{\text{beam}}$ in this analysis. The values of x_E and z can differ significantly for events with initial state radiation or hard gluon radiation. Furthermore, our use of the parton shower event generator instead of the matrix element method in LUND 7.3 makes an interpretation of the ϵ's in terms of QCD not straightforward. In spite of this disadvantage, we used the parton shower event generator because a better agreement between the data and the Monte Carlo simulation can be achieved for various event-shape distributions of multihadron events when the parton shower event generator rather than the matrix element method is used.

IV. AMY DETECTOR

AMY is a compact cylindrical detector based on a 3-T solenoid superconducting magnet and is optimized for lepton identification. Figure 1 shows a cross-sectional view of the detector. Charged particles are detected by a vertex (VTX) chamber and an inner tracking chamber (ITC), both made of straw tubes, and a cylindrical drift chamber (CDC) over the polar angle range $|\cos\theta| < 0.87$ with a momentum resolution of $\Delta p_t/p_t \sim 0.7\% \times p_t(\text{GeV}/c)$ [5]. Neutral particles are detected by a finely segmented cylindrical shower counter (SHC) over the angular range of $|\cos\theta| < 0.75$ with an energy resolution of $\sigma_E/E = 23\%/\sqrt{E(\text{GeV})} + 6\%$. The SHC is located between the CDC and the superconducting magnet coil and contains a total of 8 cm of lead ($14.5/\sin\theta$ radiation lengths; 0.46 nuclear absorption lengths). Surrounding the coil is an iron flux return yoke, which together with the coil and SHC constitutes a 1.65 m iron-equivalent hadron filter (9.8 nuclear absorption length). Outside the iron is the muon (MUO) detector system, details of which are described in the next section.

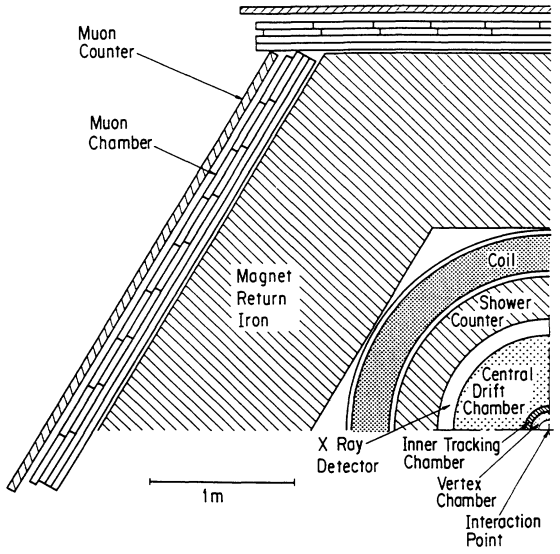

FIG. 1. AMY detector. The muon detection system consists of a 1.65 m iron-equivalent hadron filter, four layers of drift chambers, and an array of scintillation counters.

Calorimeters mounted on the magnet pole tips in both end-cap regions (ESC's) measure forward Bhabha events which are used to determine the luminosity. The ESC covers from $\theta = 12°$ to 25°. Besides the ESC, another small angle counter (SAC) is located in the extremely forward direction, covering from 2° to 3°, mainly for tagging two-photon processes.

V. MUON DETECTION SYSTEM

The muon detector is composed of six sextants, covering all of 2π in ϕ and spanning $\cos\theta$ from about -0.74 to $+0.74$. Each sextant contains a muon tracking chamber and an array of scintillation counters. Tracking is performed by four layers of drift chambers. The inner two layers, 1 and 2, have wires running along the $\hat{\phi}$ direction, and thus provide z-tracking information, while the outer two layers, 3 and 4, have wires running in the $\hat{z}$ direction, and thus provide ϕ-hit information. The scintillation counters are located on the extreme outside of the detector (away from the beam) and provide time of flight information for the muon hits. The sextants are 6.5 m long, with widths of 2.8 m (sextants 4 and 6), 3.6 m (sextants 1 and 3) and 4.1 m (sextants 2 and 5).

The drift chambers are made of extruded aluminum tube modules. A module contains eight cells, each 10 cm wide and 5 cm high, arranged in two layers of four cells each as shown in Fig. 2. The cells of layers 1 and 2, and layers 3 and 4, are offset by half a cell width (5 cm) to allow for the resolution of left-right ambiguity and also to improve efficiency. Layers 1 and 2 have 64 cells each, while for layers 3 and 4, the number of cells in a sextant vary from 28 to 40.

The 100 μm diameter gold-plated tungsten anode wires are maintained at 3.1 kV, and the tube walls are at

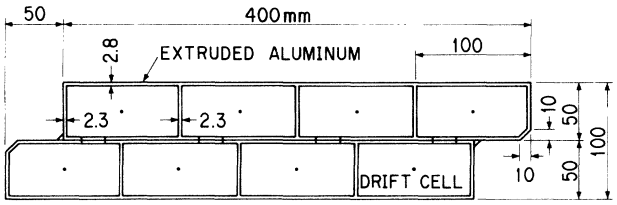

FIG. 2. A module of the muon drift chamber.

ground. P10 gas (90% Ar, 10% CH_4) is used, and is kept above atmospheric pressure by 4–5 cm of water. The average drift velocity under these conditions is about 40 mm/μsec. The position resolution obtained by this device is about 1 mm.

There are a total of 158 scintillation counters of various sizes, slightly overlapping, which completely cover the drift chambers and provide the same angular acceptance. The time of flight information which the muon counters provide is effective in removing the cosmic ray background from $e^+e^- \to \mu^+\mu^-$ selection. However, for inclusive muon events, the cosmic ray background is negligible, and we did not use the counters in this analysis.

We studied the efficiency of the muon drift chambers by collecting a large number of clean cosmic ray tracks. We determined that for $|\cos\theta| < 0.74$, the overall tracking efficiency (averaged over the sextants) is never less than 99.5%, and is usually 99.7–99.8%.

VI. ANALYSIS OF INCLUSIVE MUON EVENTS

The presence of prompt muons within hadronic jets indicates that the jets originated from either c or b quarks. The charge of each muon reflects the sign of the parent quark charge. In selecting inclusive muon events, we first imposed the following standard AMY hadronic event criteria.

(1) Five or more charged tracks with $|\cos\theta| \leq 0.85$ originating from points within $r = 5$ cm and $|z| = 15$ cm of the interaction point.

(2) Total visible energy ($E_{\rm vis}$) more than half of the total c.m. energy.

(3) Momentum imbalance along the beam direction with a magnitude less than $0.4E_{\rm vis}$.

(4) More than 5 GeV deposited in the SHC.

Then additional requirements were imposed for the presence of the muon.

(1) At least one muon hit is present. A muon hit requires a track in the muon drift chamber consisting of at least three out of a possible total of four layers.

(2) The distance between a muon hit and the extrapolated position of one of the CDC tracks (matching distance) is less than 100 cm.

(3) Momentum of the muon track is greater than 1.9 GeV/c and $|\cos\theta| \leq 0.74$.

A total of 1254 events passed the above requirements. Backgrounds to the muon signal (hadron fakes) arise principally from hadron showers in the hadron filter, where the debris reaches the muon chamber

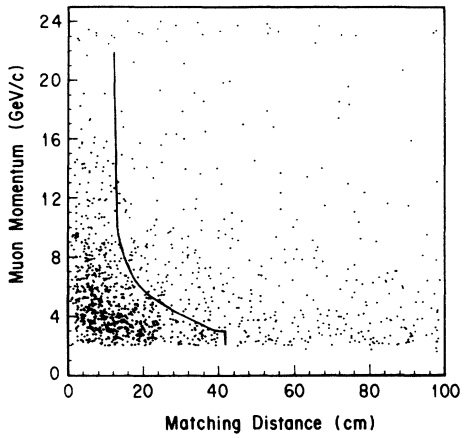

FIG. 3. Muon momentum versus matching distance for all candidate muons within a matching distance below 100 cm. The solid line curve indicates the 2σ matching distance cut.

(punchthroughs), or from the decay of $\pi^\pm$ and $K^\pm$ mesons, before they are absorbed in the hadron filter, to muons that reach the muon chamber (decay). In order to remove these backgrounds we further require that the matching distance be less than 2σ of that allowed by multiple Coulomb scattering. This requirement reduced the inclusive muon sample to 773 events. Figure 3 shows the muon momentum versus matching distance up to 100 cm for the data sample. The 2σ cut is indicated as the solid line curve in this figure.

We used Monte Carlo events to determine the CDC reconstruction efficiency for a track within a hadronic jet to be 95%. According to a study of true muons (from the $e^+e^-\mu^+\mu^-$ data sample and those in the prompt muon fraction originating from the c and b flavored hadrons in a Monte Carlo simulation), about 88% of the true muons that are reconstructed by the CDC and the muon chamber system satisfy the 2σ matching distance cut. The overall detection efficiency for muons with momenta above 3 GeV/c in the angular region of $|\cos\theta| \leq 0.74$ is 83%.

VII. $e^+e^- \to b\bar{b}$ ASYMMETRY ANALYSIS

For the determination of the forward-backward charge asymmetry for $e^+e^- \to b\bar{b}$, we assume that the yield and asymmetry of $e^+e^- \to c\bar{c}$ is correctly described by the standard model. We estimate the contributions from the $c\bar{c}$ production and the hadron fake background by using a Monte Carlo simulation, where five flavors are generated according to the standard model using the LUND 7.3 parton shower event generator [6]. As the inputs to the generator, we used the default values. We obtained the $e^+e^- \to b\bar{b}$ sample by subtracting the simulated $c\bar{c}$ signal and hadron fakes from the data. Estimation of the fraction of hadron fakes coming from b flavored hadrons requires prior knowledge of $e^+e^- \to b\bar{b}$, which is what we are trying to determine. While such a procedure may not be strictly valid, we are justified in applying it to the present case because the fraction of hadron fakes coming

from b flavored hadrons is only $\sim 1/10$ of those originating from u, d, s, and c flavored hadrons. The Monte Carlo simulation is also used for estimating the ratio of muons from b quark cascade decays to those from direct decays. This is justified because this ratio depends only on the decay kinematics of the b quark and not on the dynamics of the $b\bar{b}$ pair production. The dominant cascade decay produces muons with charge opposite to those produced by direct decay, and thus contributes oppositely to the asymmetry. We use our estimated ratio of the cascade decay to the direct decay to correct for this effect.

We define the $\theta_{\rm th}$ angle of the event as the direction of the thrust axis associated with the μ^- with respect to the incoming e^- direction. The p_T of the muon is defined as the transverse component of its momentum with respect to the thrust axis. The p_T distribution of the muons that passed the 2σ matching distance cut is shown in Fig. 4, together with the estimated contributions of $c\bar{c}$ and hadron fakes, and the $b\bar{b}$ contribution obtained by subtracting the $c\bar{c}$ estimation and hadron fakes from the data. The muons from $b\bar{b}$ extend toward higher p_T values compared with those from $c\bar{c}$ and hadron fakes. This is expected because the muons from the semileptonic decays of b flavored hadrons tend to have larger p_T values, reflecting the fact that these hadrons are heavier than those of other flavors. A Monte Carlo study indicates that we can maximize the b quark fraction by applying a cut of p_T greater than 0.7 GeV/c.

Figure 5 shows the $\cos\theta_{\rm th}$ distributions for the data, the calculations for $c\bar{c}$ and hadron fakes, and the $b\bar{b}$ signal which was obtained by subtracting the $c\bar{c}$ and hadron fakes from the data, for p_T (a) below and (b) above 0.7 GeV/c.

The $c\bar{c}$ and hadron fake contributions were calculated using a set of Monte Carlo data about five times larger than the real data. Yet statistical fluctuation of the $c\bar{c}$ contribution is not negligible and was included in our estimate of the systematic uncertainty. The

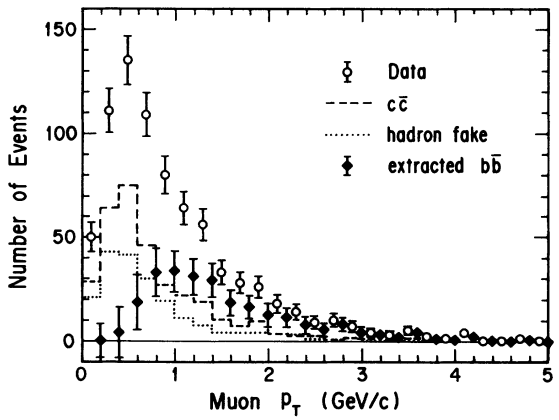

FIG. 4. The muon p_T distribution for the 773 inclusive muon candidate events that passed the 2σ matching distance cut (white dots). $c\bar{c}$ (dashed line) and hadron fakes (dotted line) contributions estimated by a Monte Carlo calculation, and the $b\bar{b}$ contribution (dark dots) obtained by subtracting $c\bar{c}$ and hadron fakes from the data, are shown separately.

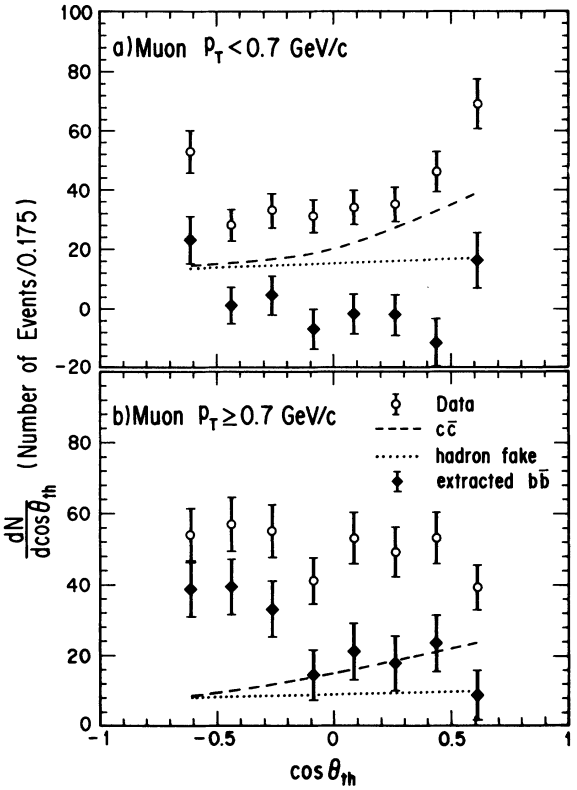

FIG. 5. The angular distribution $dN/d\cos\theta_{\rm th}$ for the 773 inclusive muon events, (a) for p_T below 0.7 GeV/c, and (b) for above 0.7 GeV/c. Contributions from $c\bar{c}$, hadron fakes, and $b\bar{b}$, were obtained as described in Fig. 4.

estimated hadron fakes amount to about 25% of the data sample after the 2σ cut, of which about 60% are punchthroughs and about 40% are decays. Even though our punchthrough calculation, which is based on the GHEISHA program [7], agrees well with available experimental data for pions, data for kaons are not available in our energy range. We estimate that about half of the punchthroughs are induced by K^+ mesons, mainly because of its smaller absorption cross section in the iron. This is a main source of systematic uncertainty in this analysis. Both the $c\bar{c}$ contribution and the hadron fake background in Fig. 5 are shown as smooth curves. However, the actual subtractions were performed using unsmoothed numbers.

We can obtain the cross section R_b and asymmetry A_b of $e^+e^- \to b\bar{b}$ from observed $dN/d\cos\theta_{\rm th}$ in the region $p_T \geq 0.7$ GeV/c by two methods. One method is to perform a χ^2 fit on the $dN/d\cos\theta_{\rm th}$ with R_b and A_b in the Monte Carlo generator as free parameters. The other method is to convert the observed $dN/d\cos\theta_{\rm th}$ into the $d\sigma/d\Omega$ and fit to Eq. (13). We applied the latter method in this study. The conversion is done by first correcting for (i) the effect of different θ definitions, (ii) the efficiency for detecting the b quark by requiring a muon, (iii) the effect of the cascade decays, (iv) the muon detection efficiency of 83%, and then normalizing to the luminosity. We obtained a θ-dependent correction factor by dividing a Monte Carlo generated $e^+e^- \to b\bar{b}$ angular distribution,

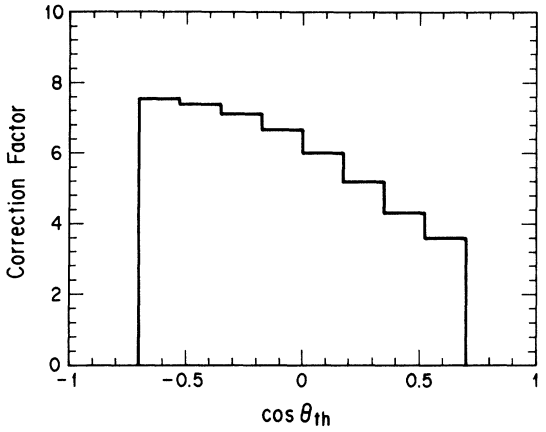

FIG. 6. Correction factor which converts $dN/d\cos\theta_{\rm th}$ for inclusive muon events, for p_T above 0.7 GeV/c into $d\sigma/d\Omega$ for $e^+e^- \to b\bar{b}$.

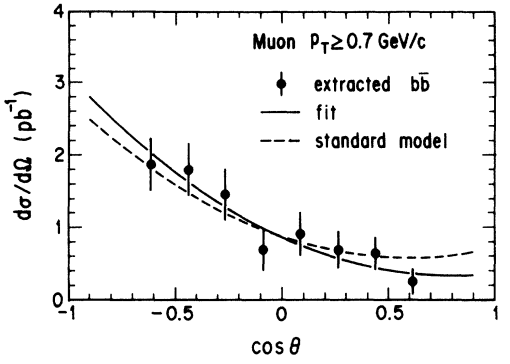

FIG. 7. Differential cross section $d\sigma/d\Omega$ of $e^+e^- \to b\bar{b}$ with the results of the fit. The standard model prediction including the effect of $B^0\bar{B}^0$ mixing is also shown.

where θ is defined as the angle between the outgoing b quark and the incoming e^- direction, by a Monte Carlo distribution equivalent to $dN/d\cos\theta_{\rm th}$. The distribution in the numerator was generated with only the Born term except the input asymmetry was varied, and with initial state radiation turned off. The distribution in the denominator was obtained from a detector simulation that takes into account full electroweak processes and QCD effects using the same input asymmetry as used in the numerator. The correction factor has a θ dependence that depends on an input asymmetry. We determined the input asymmetry for calculating the correction factor from the relation between the input asymmetries in the Monte Carlo generator and the resulting output asymmetries in the $dN/d\cos\theta_{\rm th}$ distribution. It should be noted that the output asymmetries used here have significance only as a parameter for indicating how the input asymmetries affect the $dN/d\cos\theta_{\rm th}$. A fit to the observed $dN/d\cos\theta_{\rm th}$ gave an output asymmetry of -0.32. This corresponds to an input asymmetry of -0.52. The correction factor obtained using this asymmetry value is shown in Fig. 6.

The resulting differential cross section for $e^+e^- \to b\bar{b}$, which was obtained by multiplying $dN/d\cos\theta_{\rm th}$ by the correction factor bin-by-bin, is shown in Fig. 7. Also plotted in the figure is the result of a fit to Eq. (13) in the region of $|\cos\theta_{\rm th}| \leq 0.7$, and the standard model prediction that includes the effect of $B^0\bar{B}^0$ mixing. The parameters obtained in the fit are $A_b = -0.59 \pm 0.09$ and $R_b = 0.57 \pm 0.06$.

The systematic errors in this analysis arise from uncertainties of the amount of hadron fake background and $c\bar{c}$ events which must be subtracted, from the p_T cut dependence, and from the uncertainty in determining the correction factor. In order to estimate the contribution due to hadron fake background and $c\bar{c}$ events, we repeated the analysis changing the luminosity by its uncertainty of $\pm 1.5\%$, the hadron fake contribution by $\pm 30\%$ (corresponding to the fraction contributed by the K^+-induced punchthroughs), and the $c\bar{c}$ contribution by 1σ of the Monte Carlo statistics. The effect of the p_T cut was studied by varying the p_T cut values from 0.5 GeV/c to 1.0 GeV/c. We recalculated the correction factor by varying the measured asymmetry value by $\pm 1\sigma$, and using them as the Monte Carlo inputs, calculated the $d\sigma/d\Omega$. This was used to estimate the systematic error due to the correction factor. The estimated systematic errors are summarized in Table I.

Our final results measured at a c.m. energy of $\sqrt{s}$=57.8 GeV are $A_b = -0.59 \pm 0.09 \pm 0.09$ and $R_b = 0.57 \pm 0.06 \pm 0.08$, where the first and the second errors are statistical and systematic, respectively. The effect of $B^0\bar{B}^0$ mixing is to reduce the asymmetry given by the

TABLE I. Estimates of systematic errors in the analysis of $e^+e^- \to b\bar{b}$ cross section and asymmetry. MC denotes Monte Carlo.

Error sources	Estimate of systematic errors (%)	
	A_b	R_b
Luminosity ($\pm 1.5\%$)	± 1.1	± 2.9
Hadron fake background ($\pm 30\%$)	± 5.7	± 10.4
$c\bar{c}$ background (1σ MC statistics)	± 5.0	± 6.0
p_T cut	± 8.9	± 5.1
Correction factor (1σ)	± 9.0	± 0.8
Combined systematic error	$\pm 14.8\%$	$\pm 13.4\%$

Born term into the observed asymmetry according to

$$A_b^{\rm obs} = A_b^{\rm Born}(1-2\chi). \tag{17}$$

Here $\chi = f_d\chi_d + f_s\chi_s$ contains the mixing parameters for B_d and B_s mesons, $\chi_{d(s)} = \Gamma(B_{d(s)} \to l^+)/\Gamma(B_{d(s)} \to l^\pm)$, and the fractions that a $b\bar{b}$ pair produced in the e^+e^- annihilation forms a $B_d\bar{B}_d(B_s\bar{B}_s)$ pair, $f_d(f_s)$. LEP experiments have measured χ using the production rate of same-sign dilepton events [8]. A weighted mean of the four measurements gives $\chi = 0.126 \pm 0.014$. Taking this into account, the standard model predicts the observed asymmetry to be $A_b = -0.43$. Thus our new result is about 1.3σ larger than the prediction. The result of R_b is in good agreement with the standard model prediction of 0.56.

VIII. FRAGMENTATION FUNCTION ANALYSIS

The two-dimensional momentum spectrum (p, p_T) of the prompt muons depends on the ratio of $b\bar{b}$ and $c\bar{c}$ events and on the momentum distribution that their parent heavy hadrons have before they decay semileptonically. Thus, we compare the (p, p_T) spectrum of the data with that of Monte Carlo events generated with varying parameters of the Peterson fragmentation functions. We used three p bins ($\leq$4, 4 $\sim$ 6, $\geq$6 GeV/c) and five p_T bins ($\leq$0.5, 0.5–1.0, 1.0–1.5, 1.5–2.0, $\geq$2.0 GeV/c).

The 773 inclusive muon samples were binned in 3 × 5 (p, p_T) bins. The expected distributions are described as

$$N_{\rm expect}(p,p_T) = N_{\rm bg}(p,p_T) + \Big[2N_{c\bar{c}}B_{R_c}\sum_{x_E} W_c(x_E)P_c(x_E,p,p_T) + 2N_{b\bar{b}}B_{R_b}\sum_{x_E} W_b(x_E)P_b(x_E,p,p_T) + 2N_{b\bar{b}}B_{R_c}\sum_{x_E} W_b(x_E)P_{bc}(x_E,p,p_T)\Big]. \tag{18}$$

Here $N_{\rm bg}$ are the numbers of background events in each bin, and were estimated from the Monte Carlo calculation. The first term in the brackets describes prompt muons from $c\bar{c}$ events, the next describes muons from $b\bar{b}$ events, and the last describes muons from $b \to c \to \mu$ cascade decay. $N_{c\bar{c}}$ and $N_{b\bar{b}}$ are the expected number of $c\bar{c}$ and $b\bar{b}$ hadronic events in the data. The factors of 2 indicate that the prompt muons can come from either Q or $\overline{Q}$ decay. B_{R_c} and B_{R_b} are the semileptonic branching ratios for charm and bottom hadron decay, taken to be 8.9% ± 0.86% and 10.8% ± 0.60%, respectively. The charm result is an average of CELLO, Mark J, TASSO, JADE, Mark II, and ARGUS results, where for each experiment the statistical and systematic errors were added in quadrature [10]. The bottom quark result is a recent measurement by CLEO [11].

Probabilities that heavy hadrons carrying the fractions x_E of the beam energy will yield muons in (p, p_T) space are given by $P_Q(x_E,p,p_T)$. In the case of cascade decay, $P_{bc}(x_E,p,p_T)$ gives the probability that beauty hadrons carrying x_E go through cascade decays and yield muons in (p, p_T). These probabilities, including the efficiency of detecting the muons, were estimated from a Monte Carlo calculation with a flat fragmentation function. They represent only the kinematic effects of the decays, not the dynamics of the fragmentation. We used JETSET 7.3 in this determination. We also checked the result by using both LUND 6.2 matrix element and LUND 6.3 parton shower models, and found that these probabilities do not depend on which Monte Carlo simulation is used. Physics effects are added by a weighting factor $W_Q(x_E)$, which is an integration of the Peterson fragmentation functions for each x_E bin.

The parameters ϵ_c and ϵ_b of the Peterson fragmentation function were varied to obtain the best χ^2 fit in the comparisons of the observed (p, p_T) distribution with the expected ones. The result of the fit is shown in Fig. 8. The best χ^2 was obtained for $\epsilon_c = 0.21^{+0.13}_{-0.07}$ and $\epsilon_b = 0.08^{+0.05}_{-0.04}$. These correspond to the average values of x_E of $\langle x_E\rangle_c = 0.56^{+0.04}_{-0.05}$ and $\langle x_E\rangle_b = 0.65^{+0.06}_{-0.04}$. The ratio ϵ_b/ϵ_c in this analysis gives ≈ 0.4 which is quite

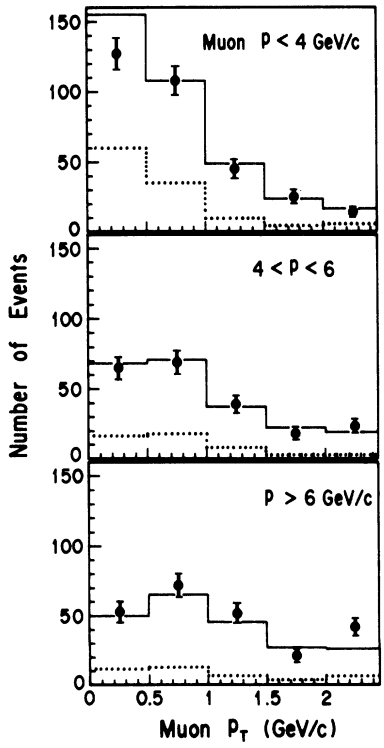

FIG. 8. The muon p_T distribution for three different muon p bins. The solid line is the result of the fit. The dotted line is the Monte Carlo estimation of hadron fake background.

TABLE II. Systematic errors of the fragmentation function analysis.

Error sources	Estimates of systematic errors (%)			
	ϵ_b	$\langle x_E \rangle_b$	ϵ_c	$\langle x_E \rangle_c$
Hadron fakes (± 30%)	+70.4	−7.2	+19.3	−3.0
	−34.0	+5.4	−17.7	+3.4
$B(b \to \mu X)(\pm 1\sigma)$	+25.6	−3.0	−5.7	+1.0
	−21.9	+3.2	−21.9	−1.0
$B(c \to \mu X)(\pm 1\sigma)$	+33.7	−3.9	+20.6	−3.2
	−21.7	+3.2	−20.6	+3.8
$R(b\bar{b})(\pm 1\sigma)$	+5.8	−0.7	−1.4	+0.2
	−5.6	+0.8	+1.3	−0.2
$R(c\bar{c})(\pm 1\sigma)$	+1.3	−0.1	+1.4	−0.2
	−1.2	+0.2	−1.4	+0.2
No first bin	−11.4	+1.6	−14.1	+2.5
Total	+82.4% −47.6%	−8.7% +7.2%	+28.9% −31.2%	−4.5% +5.8%

different from the naive prediction of 0.1 for the primordial fragmentation functions. Use of the scaling variable x_E rather than z in this analysis makes any QCD-based interpretation of ϵ parameters meaningless. Instead the results presented here are experimentally straightforward with minimum theoretical biases.

As sources of systematic errors, we considered (1) a ±30% uncertainty in the hadron fake background, (2) statistical fluctuations of $b\bar{b}$ and $c\bar{c}$ events in the Monte Carlo simulation, (3) uncertainties in the average semileptonic branching ratios, and (4) the effect of the first bin ($p < 4$ GeV/c and $p_T < 0.5$ GeV/c) where the background is the largest and the muon detection efficiency is near the threshold. The effect of the first bin was estimated by repeating the analysis with the first bin eliminated. Estimated systematic errors are listed in Table II. Including the systematic errors, the results we obtained are $\epsilon_c = 0.21^{+0.13+0.06}_{-0.07-0.07}$ and $\epsilon_b = 0.08^{+0.05+0.06}_{-0.04-0.04}$, where the first error is statistical and the second is the systematic. These epsilon values correspond to average values of the scaling variable x_E of $\langle x_E \rangle_c = 0.56^{+0.04+0.03}_{-0.05-0.02}$ and $\langle x_E \rangle_b = 0.65^{+0.06+0.05}_{-0.04-0.06}$.

We also carried out an alternative analysis of the fragmentation functions. Because of the charge asymmetry, $b\bar{b}$ events are more likely to lead to positively charged muons in the forward hemisphere (direction of e^-), and negatively charged muons in the backward hemisphere. Exactly the opposite is true for $c\bar{c}$ events. We used this information by subdividing our muon sample into two categories: one containing forward-going μ^- and backward-going μ^+, and the other containing forward-going μ^+ and backward-going μ^-. Each category was binned into 15 (p,p_T) bins as the previous method. Therefore we used a total of 30 bins in this method. The former category contains more $b\bar{b}$ events and less $c\bar{c}$ events. The opposite is true for the second category. Without subdividing the data sample, the prompt muons are 52% from c and 33% from b with the rest from cascade decays. In the first category, we expect 38% from c and 47% from b, whereas the second category contains 63% from c and 21% from b. The fractions of cascade decay muons in the subdivided samples do not change substantially. The results we obtained from this method

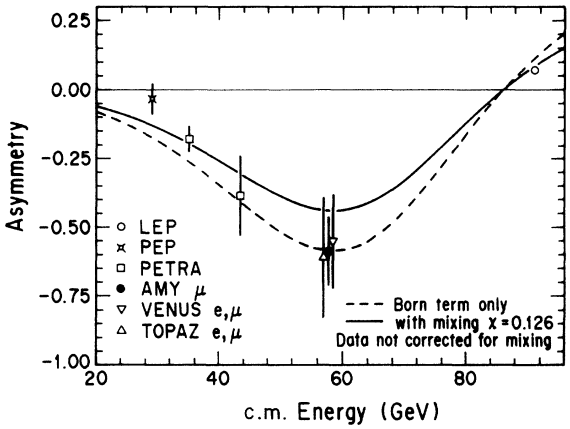

FIG. 9. The forward-backward charge asymmetry for $e^+e^- \to b\bar{b}$ as a function of the center-of-mass energy. The result of this experiment at $\sqrt{s} = 57.8$ GeV is compared with previous measurements. The solid curve is the standard model prediction including the effect of $B^0\bar{B}^0$ mixing. For comparison, the prediction without mixing is also shown as the dotted line.

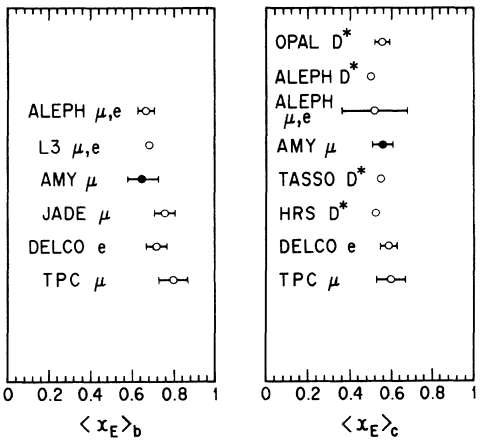

FIG. 10. The result of this experiment for the average fractions of the beam energy carried by the heavy hadrons, $\langle x_E \rangle_c$ and $\langle x_E \rangle_b$, are compared with previous measurements.

are $\langle x_E \rangle_c = 0.57^{+0.04+0.03}_{-0.04-0.03}$ and $\langle x_E \rangle_b = 0.61^{+0.06+0.04}_{-0.05-0.03}$, in good agreement with the 15-bin method.

IX. DISCUSSION

We have extracted the cross section and charge asymmetry of $e^+e^- \to b\bar{b}$, and the average x_E in the fragmentation function for c and b quarks from e^+e^- annihilation multihadron events including muons at a center-of-mass energy of 57.8 GeV/c. The results reported here are based on the total integrated luminosity of 142 pb^{-1}. While the R_b value agrees well with the standard model, we observe a small discrepancy in A_b. Our newly observed value is about 1.3σ larger than the standard model prediction. Figure 9 compares this result with previous measurements [9]. The solid line in the figure is the standard model prediction with the effect of $B^0\bar{B}^0$ mixing. The dotted line represents the expectation without mixing. It can be noticed that all three TRISTAN measurements yield a somewhat larger asymmetry. When they are combined, the value of A_b becomes -0.58 ± 0.09, which is about 2σ larger than the standard model. At this moment we are unable to conclude whether or not this is a significant effect. The $\langle x_E \rangle_c$ and $\langle x_E \rangle_b$ that we measured are in good agreement with the previous measurements reached at the SLAC e^+e^- storage ring PEP, DESY e^+e^- collider PETRA, and LEP energies [12]. They are summarized in Fig. 10.

ACKNOWLEDGMENTS

We thank the TRISTAN staff for the excellent operation of the storage ring. In addition we acknowledge the strong support and enthusiastic assistance provided by the staffs of our home institutions. This work has been supported by the Japan Ministry of Education, Science and Culture (Monbusho) and Japan Society for the Promotion of Science, the U.S. Department of Energy and National Science Foundation, the Korea Science and Engineering Foundation and Ministry of Education, and the Academia Sinica of the People's Republic of China.

[1] AMY Collaboration, H. Sagawa *et al.*, Phys. Rev. Lett. **63**, 2341 (1989).

[2] T. Appelquist and H.D. Politzer, Phys. Rev. D **12**, 1404 (1976); A. De Rújula and H. Georgi, *ibid.* **13**, 1296 (1976); J. Jersak, E. Laermann, and P.M. Zerwas, *ibid.* **25**, 1218 (1982); S. Gusken, J.H. Kuhn, and P.M. Zerwas, Phys. Lett. **155B**, 185 (1985).

[3] M. Dine and J. Sapirstein, Phys. Rev. Lett. **43**, 668 (1979).

[4] C. Peterson *et al.*, Phys. Rev. D **27**, 105 (1983).

[5] K. Ueno *et al.*, Nucl. Instrum. Methods Phys. Res. Sect. A **323**, 601 (1992).

[6] T. Sjöstrand *et al.*, CERN Report No. CERN-TH-6488-92, 1992 (unpublished).

[7] H. Fesefeldt, Nucl. Instrum. Methods Phys. Res. Sect. A **263**, 114 (1987).

[8] L3 Collaboration, B. Adeva *et al.*, Phys. Lett. B **288**, 395 (1992); ALEPH Collaboration, D. Decamp *et al.*, *ibid.* **258**, 236 (1991); DELPHI Collaboration, P. Abreu *et al.*, *ibid.* **301**, 145 (1993); OPAL Collaboration, P. D. Acton *et al.*, *ibid.* **276**, 379 (1992).

[9] TASSO Collaboration, W. Braunschweig *et al.*, Z. Phys. C **48**, 433 (1990); HRS Collaboration, C. R. Ng *et al.*, Report No. ANL-HEP-PR-88-11 (unpublished); JADE Collaboration, E. Elsen *et al.*, Z. Phys. C **46**, 349 (1990); CELLO Collaboration, H. J. Behrend *et al.*, *ibid.* **47**, 333 (1990); MAC Collaboration, H. R. Band *et al.*, Phys. Lett. B **218**, 369 (1989); TOPAZ Collaboration, A. Shimonaka *et al.*, *ibid.* **268**, 457 (1991); TOPAZ Collaboration, K. Nagai *et al.*, *ibid.* **278**, 506 (1992); VENUS Collaboration, M. Shirakata *et al.*, *ibid.* **278**, 499 (1992); OPAL Collaboration, M. Z. Akrawy *et al.*, *ibid.* **263**, 311 (1991); ALEPH Collaboration, D. Decamp *et al.*, *ibid.* **263**, 325 (1991); L3 Collaboration, O. Adriani *et al.*, *ibid.* **292**, 454 (1992); DELPHI Collaboration, P. Abreu *et al.*, Phys. Lett. **276**, 536 (1992).

[10] CELLO Collaboration, H. J. Behrend *et al.*, Z. Phys. C **19**, 291 (1983); Mark J Collaboration, B. Adeva *et al.*, Phys. Rev. Lett. **51**, 443 (1983); TASSO Collaboration, M. Althoff *et al.*, Z. Phys. C **22**, 219 (1984); JADE Collaboration, W. Bartel *et al.*, *ibid.* **33**, 339 (1987); MARK II Collaboration, R. A. Ong *et al.*, Phys. Rev. Lett. **60**, 2587 (1988); ARGUS Collaboration, H. Albrecht *et al.*, Phy. Lett. B **278**, 202 (1992).

[11] CLEO Collaboration, S. Henderson *et al.*, Phys. Rev. D **45**, 2212 (1992).

[12] DELCO Collaboration, D. E. Koop *et al.*, Phys. Rev. Lett. **52**, 970 (1983); TPC Collaboration, H. Aihara *et al.*, Phys. Rev. D **31**, 2719 (1985); JADE Collaboration, W. Bartel *et al.*, Z. Phys. C **33**, 339 (1987); L3 Collaboration, B. Adeva *et al.*, Phys. Lett. B **261**, 177 (1991); ALEPH Collaboration, D. Decamp *et al.*, *ibid.* **244**, 551 (1990); TASSO Collaboration, W. Braunschweig *et al.*, Z. Phys. C **44**, 365 (1989); HRS Collaboration, P. Baringer *et al.*, Phys. Lett. B **206**, 551 (1989); OPAL Collaboration, G. Alexander *et al.*, *ibid.* **262**, 311 (1991); ALEPH Collaboration, D. Decamp *et al.*, *ibid.* **266**, 218 (1991).

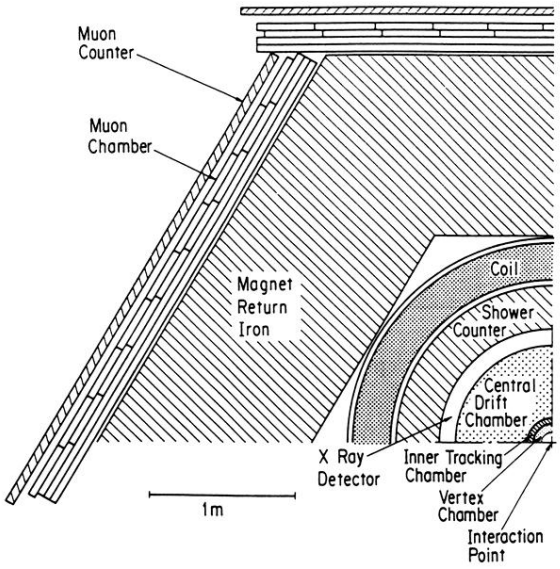

FIG. 1. AMY detector. The muon detection system consists of a 1.65 m iron-equivalent hadron filter, four layers of drift chambers, and an array of scintillation counters.